Measurement and statistical modeling of the urban heat island of the city of Utrecht (the Netherlands)

Theo Brandsma*, Dirk Wolters

Royal Netherlands Meteorological Institute, De Bilt, The Netherlands

ABSTRACT

Mobile temperature and humidity measurements have been performed along a 14 km transect through the city of Utrecht (311,000 inhabitants) in the period March 2006 - January 2009. The measurements took place on a bicycle during commuter traffic and resulted in 106 nighttime profiles (before sunrise) and 77 daytime (afternoon) profiles. It is shown how the intensity of the urban heat island depends on wind direction, cloudiness and wind speed. Statistical models are constructed that relate the mean and maximum nighttime urban heat island intensity profiles to area-averaged sky-view factors and land use combined at both the micro and local scale. Sky-view factors are estimated from a 0.5×0.5 m surface elevation database and land use is obtained from a 25×25 m land use database. The models are calibrated using the mobile measurements and provide estimates of the spatial distribution of the mean and maximum nighttime urban heat island intensity in Utrecht. Both models explain more than 75% of the variance. A separate non-linear model is introduced that relates the temperature differences between the warmest and coolest part of the transects to wind speed and cloudiness.

1. Introduction

Urban areas affect local and regional weather and air quality. With already half of the World population living in urban areas, the monitoring and modeling of these effects is increasing (Arnfield 2003; Grimmond 2006; Kanda 2007). With the resulting models society can anticipate the potential effects of plans and measures on the living conditions in urban environments.

The most known phenomenon is the urban heat island (UHI). Generally the UHI intensity increases with city size (Oke 1973). Consequently, the growth of cities may also affect temperature trends. This may occur directly, when a temperature station is situated within an (slowly) expanding city, or indirectly by advection of urban heat from an expanding city to a meteorological station downstream (Brandsma et al. 2003).

There are numerous observational studies demonstrating the existence of the UHI and many attempts to model UHI intensity using both numerical or statistical models. In studies using the statistical approach, models have been constructed that relate the UHI intensity to characteristics of the urban area, such as population, or height/width ratio of street canyons, land use, weather variables, etc.

It it known for a long time that the UHI intensity is strongly related to weather variables (Sundborg 1950; Chandler 1965; Oke 1973; Conrads 1975). Especially the importance of wind speed and cloudiness as explanatory variables is well-defined, with UHI intensity increasing with decreasing wind speed and cloudiness.

Oke (1973) found that the maximum observed UHI intensity increases about linearly with the logarithm of population size for European and North American cities, though the relationships for the two continents did not coincide. In a later publication (Oke 1981), he found a more general relationship between the maximum observed UHI intensity and the mean value of the sky-view-factor (SVF) in the central part of a city, where SVF is defined as the fraction of the visible sky from the total possible sky hemisphere at a certain location. The SVF still is the variable explaining most of the variation of the magnitude of the UHI. The height/width ratio of the street canyons in the city is sometimes used as an alternative for the SVF.

More recently, the emphasis has moved toward modeling the spatial distribution of the UHI intensity using land use parameters and geometric characteristics of the build-up area (e.g. SVF) as explaining variables (Bottyán and Unger 2003; Bottyán et al. 2005; Unger 2006; Montávez et al. 2008). In these studies often the mean maximum UHI or mean UHI intensity is considered as the dependent variable, in contrast to the maximum observed UHI intensity as defined by Oke (1973).

In this paper we attempt to further extend the statistical modeling approach. The spatial distribution of the nighttime UHI intensity of the city of Utrecht in the

Netherlands is modeled using high-resolution (1 s) multi-day mobile observations for a single transect through the city. The *SVF* and two land use parameters are used as explanatory variables. The effect of combining micro and local scale averages of the explanatory variables is investigated and a recently completed high-resolution (0.5×0.5 m) surface elevation database is used for automatically calculating estimates of the *SVF* for each location in the city. In addition, the effect of wind speed and cloudiness on the maximum UHI intensity along the transect is studied.

In contrast to many other studies that used cars for mobile measurements, we performed mobile measurements with a bicycle. This approach was introduced by Melhuish and Pedder (1998) for observing the urban heat island of Reading, UK. The Netherlands is perfectly suited for bicycle measurements as it is almost completely flat and has a dense network of safe cycle tracks.

The UHI intensity of Utrecht was studied before by Conrads (1975) (see also Conrads and Van der Hage (1971) for initial results). The current work can be seen as an extension of this work.

2. Data and methods

2.1. Study Area

Figure 1 shows the 14 km long transect running from the western boundary of the town of Nieuwegein (61,000 inhabitants) through the city of Utrecht (311,000 inhabitants) to the KNMI building near the southern border of the town of De Bilt (42,000 inhabitants).

The city of Utrecht (city center at 52°05′N, 05°07′E) is situated in the center of the Netherlands. The whole study area is flat and situated on average 2 m above mean sea level. Land use outside the build-up areas is predominantly pasture. The climate is typical for the mid-latitudes with prevailing westerly winds and precipitation for 7% of the time amounting to about 800 mm per year. Annual mean air temperatures are around 10°C, with the monthly average daily minimum temperature varying between −0.1°C (February) and 12.5°C (July) and the monthly average daily maximum temperature varying between 5.2°C (January) and 22.3°C (August).

2.2. Instrumentation

The measurements were made with an Elpro datalogger (Ecolog TH1) with two external sensors: a combi-sensor for temperature/humidity, protected by a filter, and a NTC temperature drop probe with a diameter of 2.5 mm. To protect the sensors from radiation and rain, they were mounted into a round white plastic multi-plated screen with a diameter of 85 mm and a height of 106 mm. A special device was constructed to place the instrument on the front of the bike (see Figure 2). The sensors were at a height of 1.14 m above the surface. The resolution of the temperature and the relative humidity measurements was 0.1°C and 0.1%, respectively. The accuracy of the temperature sensors equaled ±0.2°C and of the relative humidity sensor ±1.5%. For a ventilation rate of 1 m s^{-1} Elpro specified a response time of the combi-sensor of 109 s and for the NTC temperature drop probe of 16 s. The response time under field conditions, with the sensors mounted in the radiation screen and a bike speed of 5–6 m s^{-1}, could be estimated from the measurements themselves. A bicycle tunnel in Nieuwegein, at about 1.5 km from the start of the transect, often produced a positive spike in the observations. The time it took to decrease the spike magnitude with 63%, after leaving the tunnel, was considered as the response time under field conditions. The in this way estimated response times for the combi-sensor and NTC temperature probe were 30 s and 3 s, respectively.

Figure 2: Mounting of the instruments in front of the bike. The orange part is the datalogger with a display, the temperature and humidity sensors are in the multi-plated screen. The GPS is visible on the horizontal bar of the bike.

The sensors underwent a standard calibration by Elpro. In addition, the sensors were calibrated in the KNMI calibration lab at the start and end of the experiment. The differences between the calibration values before and after the experiment were negligible as were the differences between the values of the manufacturer and KNMI.

The datalogger was used to measure temperature and

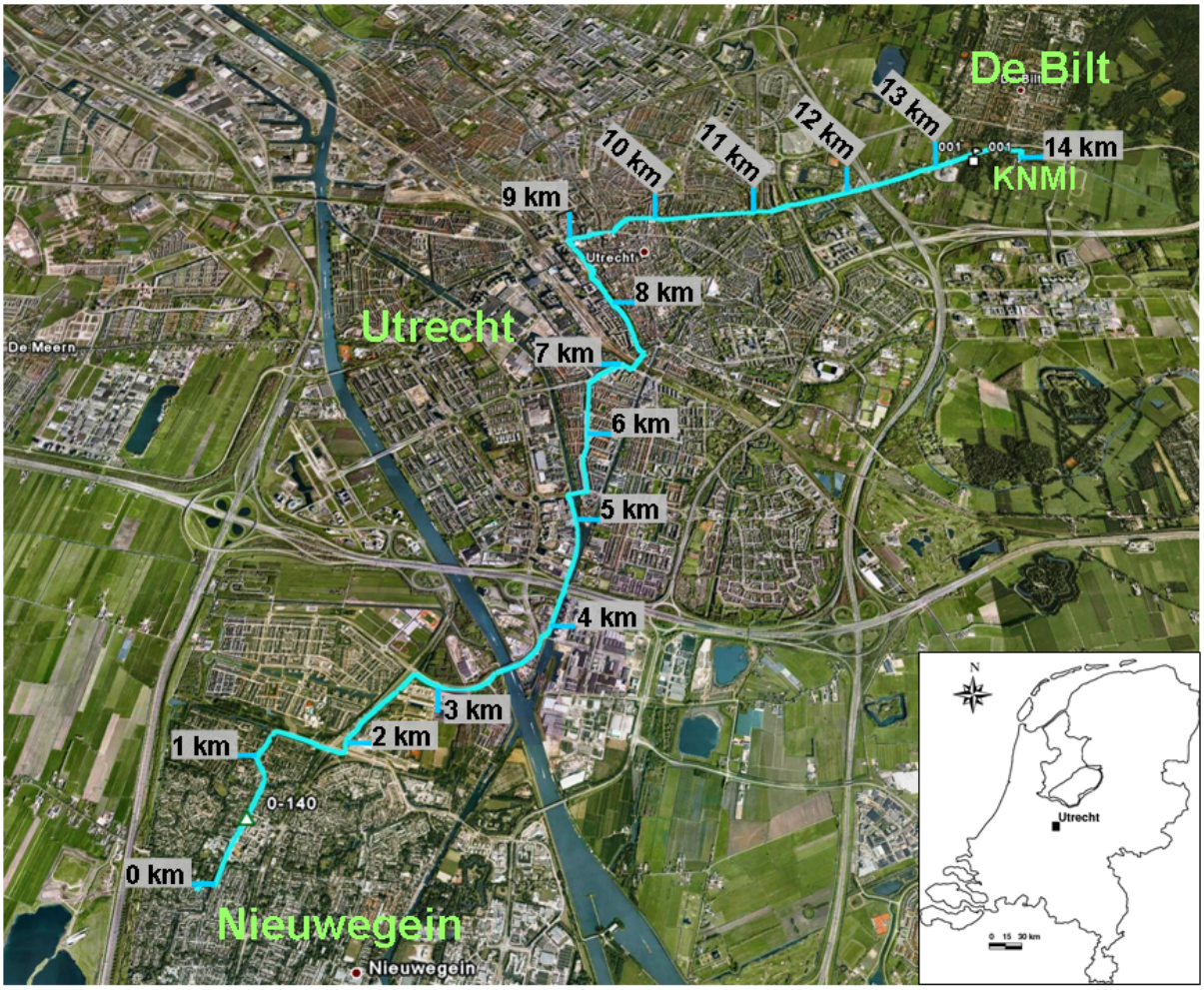

Figure 1: The 14 km long transect Nieuwegein-Utrecht-De Bilt (KNMI). The inset shows the position of Utrecht in The Netherlands.

humidity with a frequency of 1 s^{-1} (the highest available frequency of datalogger). The position of each measurement was determined with a Garmin bicycle GPS (Edge 205). The GPS was used to log the positions with a frequency of 1 s^{-1}.

2.3. Measurements

The measurements were taken in the period March 2006 - January 2009 during commuter traffic and resulted in 106 nighttime profiles (before sunrise) and 77 daytime (afternoon) profiles. The measuring days were chosen randomly and may be considered representative for the mean climatology. The average time needed for the early morning transects (Nieuwegein-Utrecht-De Bilt) was 37.3 min (average driving speed 6.3 m s^{-1}). To ensure arrival at KNMI before sunrise, the earliest starting time was 04:40 hours LT in the month of June. The average time needed for the afternoon transects (De Bilt-Utrecht-Nieuwegein) was 41.3 min (average driving speed 5.6 m s^{-1}).

About 10-minutes before the start of the measurements, the bicycle with the instruments was exposed to the outside conditions. The datalogger and GPS were synchronized at the start of the measurements. The data of both instruments were combined afterwards. To make the transects mutually comparable, a representative route was determined with fixed points every 10 m for both the early morning and afternoon transect. The morning route differs slightly from the afternoon route because of the obligation to bike on the right side of the roads, which are mostly equipped with special bike-ways on both sides. The differences in length of the two routes was negligible. The measurements (on average 1.7 per 10 m) of each transect were sampled such that each 10 m point received values of the three measurements (two for temperature and one for

relative humidity). This was done by selecting the values of the nearest measurement.

Operational measurements of wind direction, wind speed (at 1.5 m height) and cloudiness at the KNMI observatory in De Bilt were used to assess the impact of these variables on the shape and magnitude on the UHI. During conditions of heavy rain (about 5% of the time) no measurements were performed.

The temperature profiles were corrected for the diurnal cycle using the mean of the simultaneous temperature measurements of the three nearby KNMI stations Cabauw (19 km southeast of Utrecht), Herwijnen (28 km south), and Deelen (52 km east). These rural stations can be considered insensitive to the UHI of Utrecht. The spatial climatological differences of the background climate of the study area are of the order of 0.1° C and can be neglected. Spikes produced by tunnels were filtered out from the data.

The temperature of the combi-sensor was only used for the calculation of the vapor density, in all other cases we used the temperature from the fast-responding NTC drop probe.

2.4. Model construction

1) Temperature profiles

As mentioned in the introduction, the sky-view factor (SVF) is one of the most important explanatory variables of the UHI intensity. For a given location the SVF gives the fraction of the visible sky from the total possible sky hemisphere. Here the SVF was calculated analytically using a high-resolution 0.5×0.5 m surface elevation database (Van der Zon 2011). This database is now being developed for the Netherlands. The data for the study area used here has recently been completed. As an example, Figure 3 shows the visible and covered sky at a location between km makers 10 and 11. The calculation of the SVF is described in detail in Appendix A.

Besides SVFs, land use parameters are important explanatory variables. Land use parameters have been calculated here from a 25×25 m countrywide land use database (Hazeu 2005). We categorized land use into three categories: build-up, vegetation and open water.

According to the literature (Schmid 1994; Peter and Schmid 2002; Kljun et al. 2004), temperatures observed locally are affected by the surface characteristics of a larger area (the 'source area' or 'footprint'). This source area is often assumed to have a circular or elliptical shape. In the model used here, the explanatory variables were averaged over circles with radii ranging from 25 to 600 m around each location, where radii ≤ 50 m correspond to the micro scale and radii > 50 m correspond to the local scale. Land use was expressed as fractions summing up to 1. The fractions are further denoted as FB (fraction build-up), FV (fraction vegetated), and FW (fraction open water).

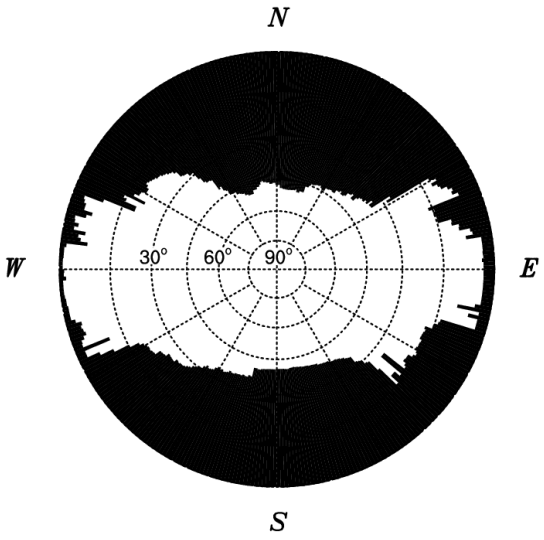

Figure 3: Example of the visible and covered sky at a location inside a typical street canyon between km makers 10 and 11 of Figure 1 as calculated from the 0.5×0.5 m surface elevation database. The dotted circles represent the sky dome.

The following model is proposed to describe the temperature profiles:

$$T' = \alpha_0 + \alpha_1 SVF_{r_1} + \alpha_2 FB_{r_1} + \alpha_3 FW_{r_1} + \alpha_4 SVF_{r_2} + \alpha_5 FB_{r_2} + \alpha_6 FW_{r_2} + \epsilon \quad (1)$$

where T' is the temperature at point of the transect (expressed as anomaly with respect to the profile mean temperature), $\alpha_i (i = 0, \ldots, 6)$ are the coefficients to be estimated, r_1 and r_2 are the radii for which the mean of the corresponding variable has been calculated, and ϵ is a zero mean error term. Because $FB+FV+FW = 1$, one of them can be omitted from the equation. Here FV was omitted.

2) Maximum nighttime urban heat island

The temperature difference between the warmest and coolest part of the transect is an important measure for the UHI intensity. Here we define the maximum nighttime temperature difference $\mathrm{UHI_{max}}$ for a certain nighttime temperature profile as the difference of the median of the twenty highest temperatures along the profile and the median of twenty lowest temperatures. In practice this mostly implies the comparison of the warmest 200 m of the transect with the coolest 200 m. The use of the median filters out incidental spikes (e.g. by the nearby passing of a bus).

It is known that wind speed and cloud cover are the most important explanatory variable for $\mathrm{UHI_{max}}$ along a given transect. The relationship between between $\mathrm{UHI_{max}}$ and wind speed is strongly non-linear (Oke 1973; Conrads

1975) (see also Figure 7). Here we propose a parametric non-linear model that relates the nighttime observations of $\mathrm{UHI}_{\max}$ to wind speed and cloudiness.

Before fitting a parametric non-linear model, we used locally weighted regression (Cleveland and Devlin 1988), also denoted loess, to find an estimate of the minimum value of the residual standard error (RSE) that could possibly be obtained by fitting a parametric model. The loess is a procedure for fitting a regression surface to the data through multivariate smoothing. The following model was fitted:

$$\mathrm{UHI}_{\max} = g(W, N) + \epsilon \tag{2}$$

where g signifies the regression surface, W is wind speed in m s^{-1}, N is cloudiness in octa's ranging from 0 (clear sky) to 8 (completely overcast) and ϵ is a random error. Locally quadratic fitting was used with a span of 0.75. RSE equaled 0.590°C and $R^2 = 0.80$.

After some trial and error, the following parametric non-linear model was found acceptable:

$$\mathrm{UHI}_{\max} = \frac{(\beta_1 + \beta_2 N)}{(W + 0.5)^{\beta_3}} + \epsilon \tag{3}$$

where $\beta_i (i = 1, \ldots, 3)$ are the coefficients to be estimated by nonlinear least squares regression.

3. Results of the measurements

3.1. Average temperature profiles

Figure 4 shows the average temperature anomaly profiles for both nighttime and daytime conditions. As expected, the temperature differences between the center of Utrecht (between km markers 9 and 10) and the surrounding areas are much larger for the nighttime than for the daytime conditions. If we define the magnitude of the UHI as the difference between the warmest and coolest temperatures along the transect, the magnitude is about 1.5°C for the mean nighttime profiles and 0.6°C for the daytime profiles. The shape of the profiles does not change significantly with a separation in winter and summer half year (not shown). The highest temperatures were measured between 9 and 9.5 km. In the remainder of the results, we focus on the nighttime measurements only. Conrads (1975) showed that the UHI intensity of Utrecht reached its maximum around midnight and thereafter remained nearly constant until sunrise.

Figure 5 shows the average temperature anomaly profiles for four wind direction categories. The figure shows that the shape of the profiles differs from direction to direction. The shapes for the west and south categories are comparable. The same holds for the shapes of the east and north categories. The differences in the shapes of the temperature profiles may (partly) be caused by the advection of urban heat. Note for instance that for the west and south categories the temperature outside of the city of Utrecht (between km markers 11 and 14) continues going down, while for directions North and east the temperature decrease stops around km marker 12. Note further that the temperature differences between the first part of the transect in Nieuwegein (between km markers 0 and 2) and the last part of the transect in De Bilt (between km markers 13 and 14) are about 0.7°C smaller for the west and south direction than for the north and east directions. For westerly winds, this may be an indication of the advection of urban heat of Utrecht to De Bilt.

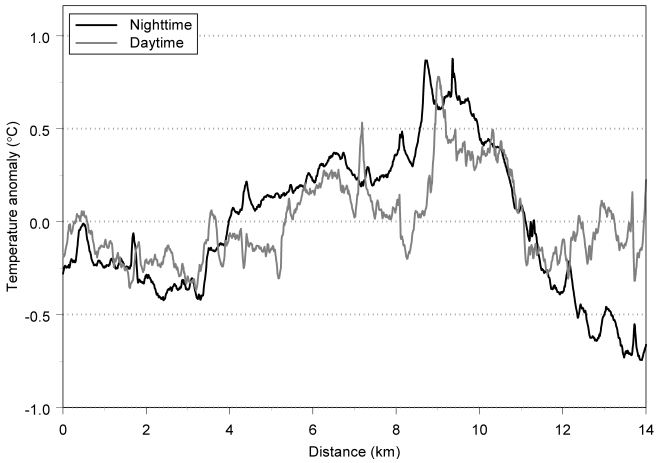

Figure 4: Average temperature anomaly profiles for nighttime (106 profiles) and daytime (77 profiles) conditions. Distance (horizontal axis) corresponds to the km markings in Figure 1. Anomalies are with respect to profile means.

3.2. Maximum temperature differences

The maximum temperature differences between the warmest part of the transect (mostly near the city center) and the surrounding countryside may be much larger than the average differences. Figure 6 shows the temperature profiles for days with $\mathrm{UHI}_{\max} > 5.0$°C. For the three days that meet this criterion (13 and 15 March 2007 and 15 February 2008), $\mathrm{UHI}_{\max}$ equaled 5.1, 5.2 and 5.4°C, respectively. These values of $\mathrm{UHI}_{\max}$ are smaller than the 7.0°C that could be expected from the relationship between $\mathrm{UHI}_{\max}$ and population size for European cities (Oke 1973). However, it should be realized that the measurements presented here stem from a limited set of 106 profiles for a fixed transect, which does not necessarily contain the warmest part of the center of Utrecht.

For all three profiles, the average wind speed during the rides was < 0.4 m/s. On 13 March 2007 and 12 February 2008 there were clear-sky conditions, while on 15 March 2007 the conditions changed from cloudy to clear-sky during the ride. Wind direction was northwest on 13 March

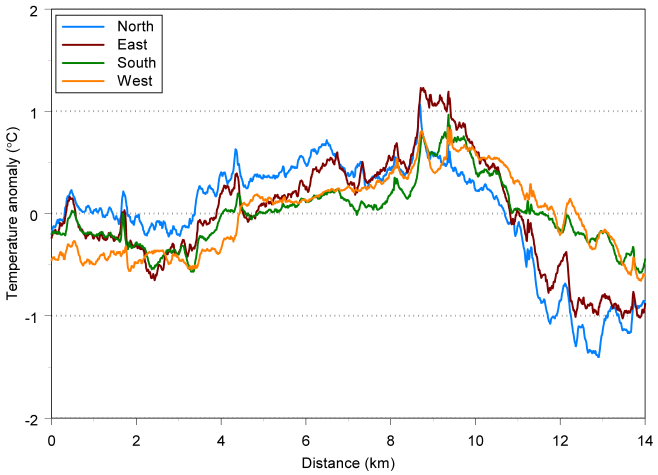

Figure 5: Average nighttime temperature anomaly profiles for 4 wind direction classes: north (23 profiles), east (18), south (35), west (30). Anomalies are with respect to profile means.

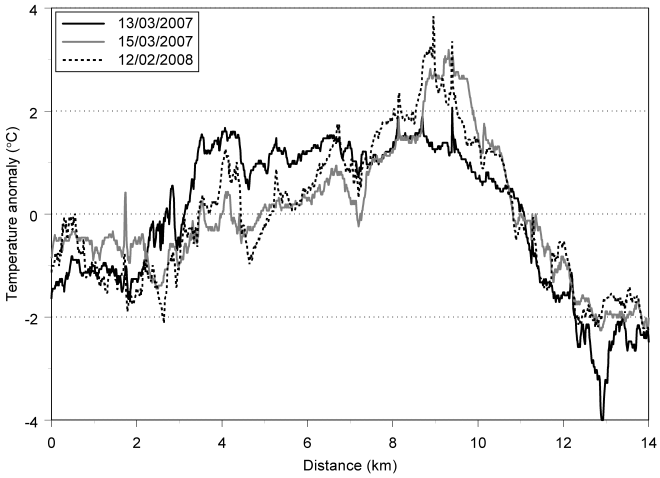

Figure 6: Temperature anomaly profiles for the 3 days with the largest nighttime temperature differences between the warmest and coldest part along the transect. Anomalies are with respect to profile means.

2007, southeast on 15 March 2007 and northeast on 12 February 2008.

Figure 7 shows the dependence between the maximum temperature differences $\mathrm{UHI_{max}}$ and wind speed for two cloudiness categories. The figure clearly shows that the largest differences occur at small wind speeds (< 1 m s^{-1}) and few clouds. This is in agreement with other studies, see e.g. Morris and Plummer (2001). Also the non-linearity of the relationship is clear.

Although the weather conditions, expressed in wind speed and cloudiness, are the main factor explaining the day-to-day variations in the magnitude of $\mathrm{UHI_{max}}$ (Figure 7) and the shape of the profiles (Figure 6), there may also be reasons for deviations. First, cloudiness is measured at the end of the transect at KNMI in De Bilt and may not always be representative for the rest of the transect. In addition, cloudiness is measured automatically with a laser ceilometer which looks only vertically upward and not to the surroundings. Second, the magnitude of $\mathrm{UHI_{max}}$ (and thus the shape of the temperature profiles) is to a large extent determined by wind speed, where low wind speeds (say < 0.5 m/s) cause large $\mathrm{UHI_{max}}$. The measurement of low wind speeds with cup anemometers faces, however, some difficulties because of the existence of threshold speeds (the wind speed that is needed to get the cups rotating). A known phenomenon of cup anemometers is that the threshold wind speed increases with time. Third, besides wind speed and cloudiness at the time of the measurements, antecedent conditions may also affect $\mathrm{UHI_{max}}$. Finally, we noticed that relatively large values of $\mathrm{UHI_{max}}$ may sometimes occur during conditions of fog measured at KNMI. For these conditions, the large temperature differences between the city and rural area might also partly be caused by spatial fog differences caused by the city.

3.3. Average vapor density profiles

Vapor density ρ_v was calculated from the relative humidity and temperature measurements of the combi-sensor (WMO 2008). Figure 8 shows the average ρ_v profiles for the nighttime and daytime profiles. The figure shows that the averages of both profiles are close to each other but that the shapes differ. The daytime profile clearly shows that the city of Utrecht causes a decrease in the amount of moisture with respect to the surrounding countryside. This is probably related to the relatively small evaporation values in the city. As could be expected on the basis of the literature, the differences are small (Hage 1975). The lack of nighttime variation suggest that vapor density does not play an important role in explaining the variation of the nighttime UHI intensity profiles.

4. Results of the urban heat island modeling

The model in equation 1 (Section 2.4) was applied to the following 2 variables: (1) the mean nighttime UHI intensity as shown in Figure 4, and (2) the maximum nighttime UHI intensity, defined here as the mean of the 3 profiles shown in Figure 6. The model in equation 2 was applied to $\mathrm{UHI_{max}}$ as presented in Figure 7 and defined in Section 2.4.

The purpose of the model in equation 1 is to obtain an estimate of the spatial distribution of the mean and maximum nighttime UHI intensity of the city of Utrecht. The model is fitted using the high-resolution data along the

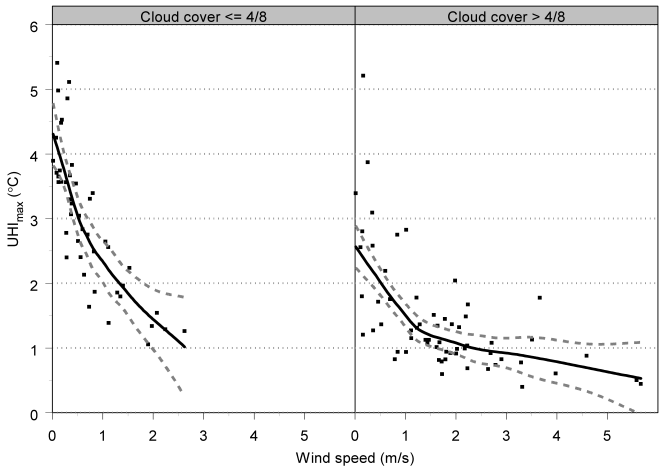

Figure 7: Relationship between the maximum temperature differences $\mathrm{UHI}_{\max}$ (nighttime) between the warmest part of the profiles (center of Utrecht) and the coldest parts (surrounding countryside) as a function of wind speed for situations with little cloud (cloud cover $\leq 4/8$) and much cloud (cloud cover $> 4/8$). The smooth lines are the result of fitting of a regression surface to the data through multivariate smoothing (loess) (Cleveland and Devlin 1988). The gray dashed curves give the point-wise 2 times standard-error bands.

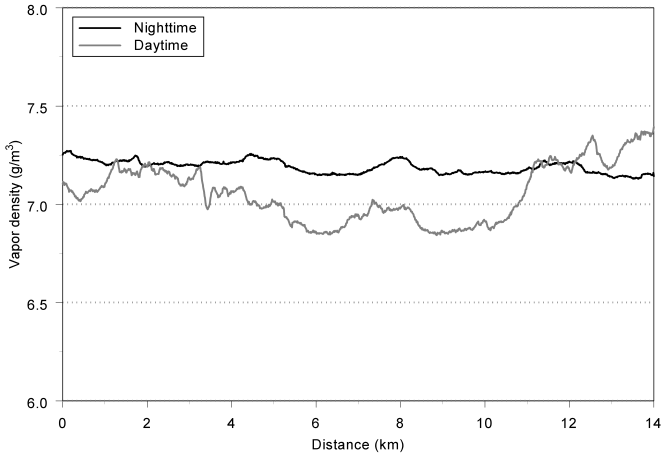

Figure 8: Average vapor density profiles for the morning (69 profiles before sunrise) and afternoon measurements (47 profiles).

transect. The spatial availability of the explanatory variables then allows to obtain areal estimates of the mean and maximum UHI intensity for the city and its surroundings. The model in equation 2 explicitly describes the relationship between $\mathrm{UHI}_{\max}$ and wind speed and cloudiness. In combination with the first model, this model may be used to obtain first order estimates for the nighttime UHI intensity for all combinations of winds speed and cloudiness.

4.1. Model for the mean nighttime UHI intensity

The model in Equation 1 was fitted to the mean nighttime UHI intensity (mean of the 106 nighttime profiles as shown in Figure 4, 1403 data points). Table 1 compares R^2 for several combinations of r_1 and r_2. The table shows results for cases with and without using a weight function. With the weight function, the weights decrease linearly with the distance to the location of interest. The differences between weighted and non-weighted are generally small. The non-weighted combinations seem to converge faster to an optimal model (in terms of R^2) than the weighted cases. We therefore choose the non-weighted alternative with $r_1 = 50$ and $r_2 = 400$ m.

Tabel 2 presents the coefficients of the model and their significance. The intercept is not significantly different from zero and is omitted in the final model estimation. The final model can be written as:

Table 1: Comparison of models with several combinations of r_1 and r_2 in Eq.1

	R^2	
(r_1, r_2) (in m)	weighted	non-weighted
(25,100)	0.632	0.646
(25,200)	0.758	0.774
(25,300)	0.800	0.814
(25,400)	0.810	0.816
(25,500)	0.812	0.809
(25,600)	0.811	0.807
(50,100)	0.643	0.647
(50,200)	0.760	0.775
(50,300)	0.798	0.812
(50,400)	0.809	0.817
(50,500)	0.814	0.814
(50,600)	0.815	0.815

$$\begin{aligned}\hat{T}' = &-0.463SVF_{50} + 0.270FB_{50} \\ &+0.358FW_{50} - 1.012SVF_{400} \\ &+1.032FB_{400} + 0.764FW_{400}\end{aligned} \quad (4)$$

where $\hat{T}'$ is the modeled temperature (anomaly with respect to the profile mean). From the equation and Table 2 it is clear that the explanatory variables for $r = 400$ m have a much stronger effect on temperature than those for $r = 50$ m. In fact, the model with only the variables for $r = 50$ m explains 49.7% of the variance, while the model with only the variables for $r = 400$ m explains 79.3% of the variance. The value of adding the explanatory variables for $r_1 = 50$ m compared to using only the variables for $r_2 = 400$ m is thus rather limited. Nonetheless, all parameter estimates for the explanatory variables are highly significant.

Table 2: Parameter estimates for the model in Equation 1 with $r_1 = 50$ m, $r_2 = 400$ m and $R^2 = 0.817$ for the mean nighttime UHI intensity.

	value	st.error	t-value
$\hat{\alpha_0}$	-	-	-
$\hat{\alpha_1}$	–0.463	0.051	–9.073
$\hat{\alpha_2}$	0.270	0.027	10.083
$\hat{\alpha_3}$	0.358	0.037	9.723
$\hat{\alpha_4}$	–1.012	0.055	–18.464
$\hat{\alpha_5}$	1.032	0.021	48.781
$\hat{\alpha_6}$	0.764	0.065	11.808

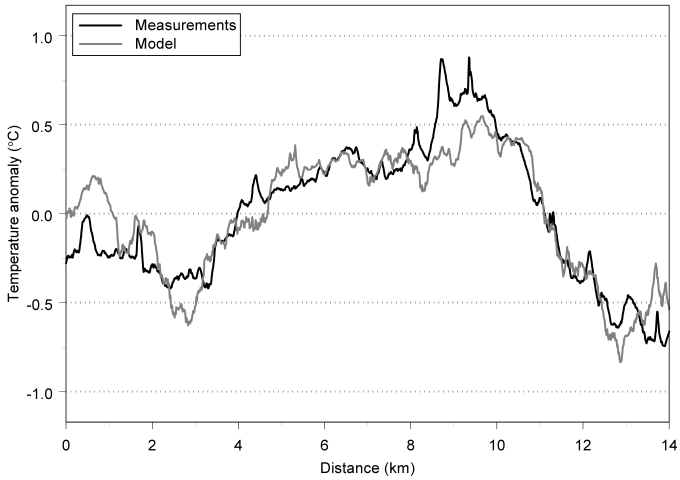

Figure 9: Comparison of the measured and modeled mean nighttime UHI intensity. Anomalies are with respect to profile means.

Figure 9 compares the measured and modeled temperatures. The figure shows that the modeled temperatures not always follow the measured temperatures. The residual standard error of the model equals 0.164°C. The deviations between measured and modeled temperatures are acceptable with respect to the residual standard error.

Equation 4 can now be used to calculate the areal distribution of the mean nighttime UHI intensity. For 2-dimensional presentation purposes it is often convenient to express the UHI intensity as the surplus of the temperature in the urban area to the temperature of the rural background temperature. Here we assume the rural temperature to be equal to the lowest model temperature in the 2-dimensional grid. Subtracting this value from the right-hand side of Equation 4 yields the mean nighttime UHI intensity with respect to the rural background temperature.

Figure 10 shows the areal distribution of the UHI intensity as defined above. The figure clearly shows the warm and cool places in and around Utrecht, where the warm

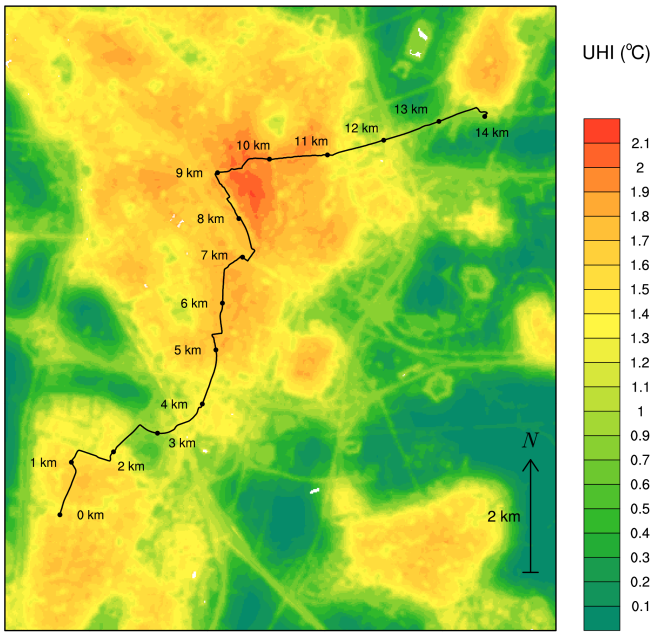

Figure 10: Spatial distribution of the mean nighttime UHI intensity for the city of Utrecht and its surroundings as calculated from the model in Equation 4 with respect to the rural background temperature. The black curve is the transect.

places correspond to the build-up area and the cool places to the rural area, consisting mainly of grassland. It is also visible that the transect almost crosses the warmest location in the city, which corresponds to the historical center of Utrecht. This area is partly closed for traffic. The large highways surrounding the city and the junctions are also visible, being somewhat warmer than the surrounding rural areas.

4.2. Model for the maximum nighttime UHI intensity

The model in Equation 1 was also fitted to the maximum nighttime UHI intensity (mean of the 3 profiles shown in Figure 6, 1403 data points). We used the same values for r_1 and r_2 as found for the mean nighttime UHI intensity ($r_1 = 50$ m, $r_2 = 400$ m).

Tabel 3 presents the coefficients of the model and their significance. The resulting model is:

$$\begin{aligned}\hat{T'} = -0.823 - 2.008SVF_{50} + 0.301FB_{50} \\ +0.584FW_{50} - 1.523SVF_{400} \\ +3.754FB_{400} + 5.183FW_{400}\end{aligned} \quad (5)$$

The model explains about 76% of the variance, which is somewhat smaller than that for the mean UHI intensity but still satisfactory. As could be expected, the absolute values

Table 3: Parameter estimates for the model in Equation 1 with $r_1 = 50$ m, $r_2 = 400$ m and $R^2 = 0.759$ for the mean nighttime UHI intensity.

	value	st.error	t-value
$\hat{\alpha_0}$	–0.823	0.269	–3.056
$\hat{\alpha_1}$	–2.008	0.195	–10.309
$\hat{\alpha_2}$	0.301	0.104	2.903
$\hat{\alpha_3}$	0.584	0.142	4.120
$\hat{\alpha_4}$	–1.523	0.330	–4.618
$\hat{\alpha_5}$	3.754	0.124	30.213
$\hat{\alpha_6}$	5.183	0.272	19.078

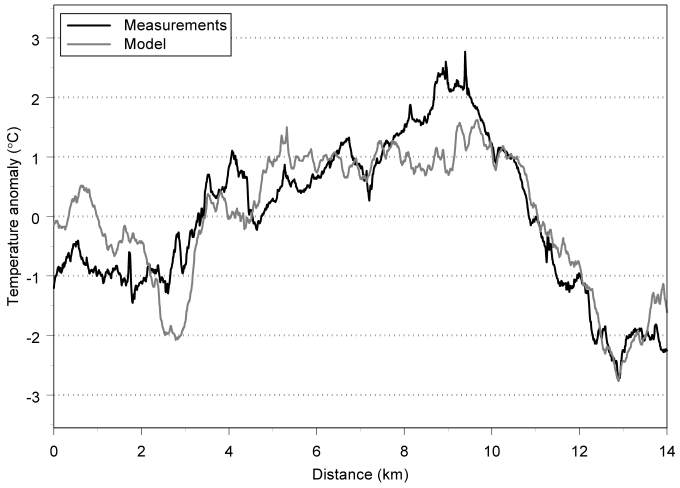

Figure 11: Comparison of the measured and modeled maximum nighttime UHI intensity (mean of the 3 profiles shown in Figure 6). Anomalies are with respect to profile means.

of the coefficients in Table 3 are larger than the corresponding values in Table 2. Note that, compared to the model for the mean UHI intensity, SVF_{50} becomes a stronger predictor than SVF_{400}. This seems physically plausible as the maximum UHI intensities occurs with low wind speeds and clear-sky conditions. During these stable conditions small scale phenomena become important.

The model with only the variables for $r = 50$ m explains only 46.2% of the variance while the model with only the variables for $r = 400$ m explains 73.7% of the variance. Again, the advantage of adding the explanatory variables for $r_1 = 50$ m compared to using only the variables for $r_2 = 400$ m is limited.

Figure 11 compares the measured and modeled temperatures. As in Figure 9, the figure shows that the modeled temperatures not always follow the measured temperatures. Here the residual standard error of the model equals 0.627°C. Again, the deviations between measured and modeled temperatures are acceptable with respect to the residual standard error.

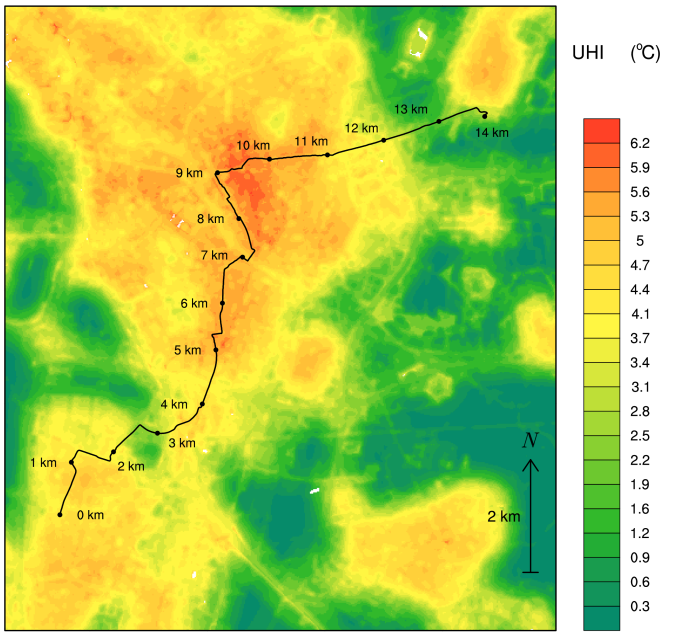

Figure 12: Spatial distribution of the maximum nighttime UHI intensity for the city of Utrecht and its surroundings as calculated from the model in Equation 5 with respect to the rural background temperature. The black curve is the transect.

Equation 5 is used to calculate the areal distribution of the maximum UHI intensity. Again we assume that the rural temperature equals the lowest model temperature in the 2-dimensional grid. Subtracting this value from the right-hand side of Equation 5 yields the maximum nighttime UHI intensity with respect to the rural background temperature.

Figure 12 shows the the areal distribution of the maximum nighttime UHI intensity as defined above. As for Figure 10, the figure clearly shows the warm and cool places in and around Utrecht, only the magnitudes are much larger now. The warmest location in the center of Utrecht has a modeled UHI intensity which is 6.24°C above the rural background. Note that the magnitudes of the maximum nighttime UHI intensity in Figure 12 are about 3 times larger than magnitudes of the mean nighttime UHI intensity in Figure 10.

4.3. Model for $\mathrm{UHI_{max}}$

Tabel 4 presents the coefficients of the model in Equation 3 and their significance. The resulting model is:

$$\widehat{\mathrm{UHI_{max}}} = \frac{(3.081 - 0.144N)}{(W + 0.5)^{0.672}} \qquad (6)$$

Table 4: Parameter estimates for the model in Equation 3 for $\mathrm{UHI}_{\max}$.

	value	st.error	t-value
$\hat{\beta}_1$	3.081	0.095	32.5
$\hat{\beta}_2$	–0.144	0.019	–7.4
$\hat{\beta}_3$	0.672	0.056	11.9

where $\widehat{\mathrm{UHI}_{\max}}$ is the modeled $\mathrm{UHI}_{\max}$. The RSE of this model equals 0.600°C which is almost equal to that of the non-parametric model (see Section 2.4). The parameters estimates are slightly correlated with the largest correlation –0.76 between the estimates of β_1 and β_2. This is, however, still acceptable. The model is able to reproduce the smooth lines in Figure 7 and can be used to estimate $\mathrm{UHI}_{\max}$ for an arbitrary combination of W and N.

The relationship for $\mathrm{UHI}_{\max}$ of Equation 6 can be used to obtain a first order estimate of the spatial distribution of the nighttime UHI intensity for an arbitrary combination of W and N. We may infer that the areal distribution of the maximum UHI intensity in Figure 12 represents the situation for $W = 0$ m s^{-1} and $N = 0$ octa (see Section 3.2). Equation 6 gives $\widehat{\mathrm{UHI}_{\max}}(W = 0, N = 0) = 4.9$°C. If we would like to know how Figure 12 would look like, e.g. for $W = 1$ m s^{-1} and $N = 3$, we can calculate $\widehat{\mathrm{UHI}_{\max}}(W = 1, N = 3) = 2.0$°C. The factor $2.0/4.9 = 0.41$ can then be used to multiply the values in Figure 12 to obtain nighttime UHI intensitity for $W = 1$ m s^{-1} and $N = 3$ octa. Because of urban heat advection, the result would be valid for average wind direction conditions only. Note again that this yields only a first order approximation. Especially with increasing wind speed, the larger scales become more important and may affect the spatial distribution of temperatures.

5. Discussion

The present study showed how a bicycle can be used for obtaining high-resolution observations of the UHI that can be used for describing and modeling the UHI intensity. This relatively cheap and efficient way of measuring the UHI intensity may be applicable for other flat urban areas as well.

Two multiple-linear regression models have been proposed to describe the mean and maximum nighttime UHI intensity profiles of the city Utrecht. The *SVF*, and the fractions of built-up and water area are meaningful predictors, which is in agreement with other results in the literature. The importance of calculating the predictors at the right scale is illustrated by combining predictors at both the micro and local scale.

In addition to the two linear models, a non-linear model is constructed that relates the temperature difference between the warmest and coldest part along the profiles to wind speed and cloudiness. We believe that the three models together, estimated with the data of Utrecht, can be applied to obtain first-order predictions for the other cities in the Netherlands as well, and probably also for flat situated cities in comparable climates.

The study focused on the nighttime UHI intensity as the UHI is most evident then. Splitting the data into seasons and/or wind direction categories might explain somewhat more of the variance of the models, and improve the fits a shown in Figures 9 and 11. However, more data would be needed in that case. A further improvement might be possible by making the shape of the source area dependent on the wind direction.

A difficult point in each UHI study is the choice of the rural reference. Because of climatological temperature differences, it is desirable to have a rural reference as close as possible to the urban area. However, in reality there is a transition zone between the urban area and the rural area whose extension depends on the advection of urban heat. The location of the boundary between the transition zone and the rural area is thus dynamic (Lowry 1977) and depends on wind direction and other weather variables. Here we used as rural reference a representative minimum temperature value along the transect (which may change from day to day) and representative minimum temperatures in the model area. For future measuring campaigns, it may be sensible to have several potential rural reference stations which, depending on the wind direction, may be used as rural reference.

The difficulty with choosing the rural reference, is one of the reasons that models of the UHI intensity, as found in the literature, are not directly comparable. Another important reason is the differences in methods for calculating predictor variables. For instance, the *SVF* may be estimated from photographic images or, as we did, from a height database leading to different values of the *SVF*. In the latter, the resolution of the height database may also influence the *SVF*.

6. Conclusions

High-resolution measurements of temperature and humidity taken on a bicycle have been used to describe and model the UHI intensity of the city of Utrecht. The mean and maximum nighttime UHI intensity could be described by a statistical model using the *SVF* and the fractions of build-up area and water area as predictors. The predictors have been calculated at the micro and local scale. The effect of combining the two scales in the models is investigated. It appeared that the nighttime UHI intensity can best be described by the predictors on the local scale. The addition of the predictors on the micro scale only slightly increases the variance explained by the model. A non-

linear model is constructed that relates the temperature difference between warmest and coldest parts along the profiles to wind speed and cloudiness. Together, the models present an easy tool to obtain first order estimates of the nighttime UHI intensity in Utrecht and probably also other cities in comparable climates.

7. Acknowledgments

We are grateful to our colleague Robert Leander for writing the software that facilitated the combining of the GPS data, the datalogger data the data of the meteorological station De Bilt. Adri Buishand is thanked for his advice on statistics and Raymond Sluiter for assistance with the use of surface elevation and land use geospatial information.

Appendix: Calculation of the *SVF*

*SVF*s were calculated using a high-resolution (0.5×0.5 m) height dataset containing the heights of buildings, vegetation, and open areas. An additional (0.5×0.5 m) ground level dataset was used to distinguish between gridpoints classified as buildings or vegetation, and open area gridpoints (such as streets, parking lots or parks). *SVF*s have been calculated on a grid of 1×1 m for the open areas only (rooftops and other elevated surfaces are thus excluded).

Here we used the vector-based method described by Gàl et al. (2007) and Matuschek and Matzarakis (2010) for the calculation of *SVF*s. For all gridpoints, the *SVF* was calculated using height information inside a circle with radius r and the location of interest in the center. First it was calculated, for every ϕ-spaced radial of this circle, which points in the (rectangular) grid lie closest, and thus, are most representative for the true locations along this radial. Next, for every radial the steepest vertical angle δ was taken, made by any object on these grid points with the horizon:

$$\delta = \max(\tan^{-1}(\frac{h_i - h_c}{d_i})) \tag{7}$$

in which h_i are the heights on grid points i along the radial, h_c is the height in the center of the circle and d_i is the distance of these grid points to the center of the circle. Next, from all angles δ along all ϕ spaced radials, 'partial' sky obstruction factors can be calculated and summed. The *SVF* is then defined as 1 minus the summed obstruction factors:

$$SVF = 1 - \sum_{n=1}^{360/\phi} sin^2\delta_n \left(\frac{\phi}{360}\right) \tag{8}$$

in which $360/\phi$ must yield an integer number.

The accuracy of the calculated *SVF*s increases with increasing radial length r and decreasing angle ϕ at the cost of sharply increasing computational demands. Above (under) certain thresholds for r and ϕ, results become insensitive to these parameters. After investigating the estimated *SVF*s using different values of r and ϕ, we took $r = 50$ m and $\phi = 2°$. The calculation of the *SVF*s for these values took for the whole study area about 450 hours on a standard Unix workstation.

REFERENCES

Arnfield, A. J., 2003: Two decades of urban climate research: a review of turbulence, exchanges of energy and water, and the urban heat island. *International Journal of Climatology*, **23 (1)**, 1–26, doi:10.1002/joc.859, URL `http://dx.doi.org/10.1002/joc.859`.

Bottyán, Z., A. Kircsi, S. Szegedi, and J. Unger, 2005: The relationship between built-up areas and the spatial development of the mean maximum urban heat island in Debrecen, Hungary. *International Journal of Climatology*, **25 (3)**, 405–418, doi:10.1002/joc.1138, URL `http://dx.doi.org/10.1002/joc.1138`.

Bottyán, Z. and J. Unger, 2003: A multiple linear statistical model for estimating the mean maximum urban heat island. *Theoretical and Applied Climatology*, **75**, 233–243, URL `http://dx.doi.org/10.1007/s00704-003-0735-7`, 10.1007/s00704-003-0735-7.

Brandsma, T., G. P. Können, and H. R. A. Wessels, 2003: Empirical estimation of the effect of urban heat advection on the temperature series of De Bilt (The Netherlands). *International Journal of Climatology*, **23 (7)**, 829–845, doi:10.1002/joc.902, URL `http://dx.doi.org/10.1002/joc.902`.

Chandler, T., 1965: *The Climate of London*. Hutchinson, 292 pp.

Cleveland, W. and S. Devlin, 1988: Locally weighted regression: an approach to regression analysis by local fitting. *Journal of the American Statistical Association*, **83**, 3–22.

Conrads, L., 1975: Observations of meteorological urban effects. The heat island of Utrecht. Ph.D. thesis, University of Utrecht, 84 pp.

Conrads, L. and J. Van der Hage, 1971: A new method of air-temperature measurement in urban climatological studies. *Atmospheric Environment*, **5 (8)**, 629–635.

Gàl, T., M. Rzepa, B. Gromek, and J. Unger, 2007: Comparison between sky view factor values computed by two different methods in an urban environment. *Acta Climatologica Et Chronologica*, 17–26.

Grimmond, C. S. B., 2006: Progress in measuring and observing the urban atmosphere. *Theoretical and Applied Climatology*, **84**, 3–22, URL http://dx.doi.org/10.1007/s00704-005-0140-5, 10.1007/s00704-005-0140-5.

Hage, K. D., 1975: Urban-rural humidity differences. *Journal of Applied Meteorology*, **14**, 1277–1283, doi:10.1175/1520-0450(1975)014⟨1277:URHD⟩2.0.CO;2.

Hazeu, G., 2005: Landelijk Grondgebruiksbestand Nederland (LGN5); Vervaardiging, nauwkeurigheid en gebruik. Alterra-report 1213, Alterra, Wageningen, the Netherlands.

Kanda, M., 2007: Progress in urban meteorology :a review. *Journal of the Meteorological Society of Japan*, **85B**, 363–383.

Kljun, N., P. Calanca, M. Rotach, and H. Schmid, 2004: A simple parameterisation for flux footprint predictions. *Boundary-Layer Meteorology*, **112**, 503–523, URL http://dx.doi.org/10.1023/B:BOUN.0000030653.71031.96, 10.1023/B:BOUN.0000030653.71031.96.

Lowry, W. P., 1977: Empirical estimation of urban effects on climate: a problem analysis. *Journal of Applied Meteorology*, **16**, 129–135, doi:10.1175/1520-0450(1977)016⟨0129:EEOUEO⟩2.0.CO;2.

Matuschek, O. and A. Matzarakis, 2010: Estimation of sky view factor in complex environment as a tool for applied climatological studies. *Berichte des Meteorologischen Instituts der Albert-Ludwigs-Universität Freiburg*, **Nr. 6**.

Melhuish, E. and M. Pedder, 1998: Observing an urban heat island by bicycle. *Weather*, **53 (4)**, 121–128.

Montávez, J. P., J. F. González-Rouco, and F. Valero, 2008: A simple model for estimating the maximum intensity of nocturnal urban heat island. *International Journal of Climatology*, **28 (2)**, 235–242, doi:10.1002/joc.1526, URL http://dx.doi.org/10.1002/joc.1526.

Morris, S. I., C. J. G. and N. Plummer, 2001: Quantification of the influences of wind and cloud on the nocturnal urban heat island of a large city. *Journal of Applied Meteorology*, **40 (2)**, 169–182, doi:10.1175/1520-0450(2001)040⟨0169:QOTIOW⟩2.0.CO;2, URL http://dx.doi.org/10.1002/joc.1526.

Oke, T., 1973: City size and the urban heat island. *Atmospheric Environment (1967)*, **7 (8)**, 769–779, doi:DOI:10.1016/0004-6981(73)90140-6, URL http://www.sciencedirect.com/science/article/pii/0004698173901406.

Oke, T. R., 1981: Canyon geometry and the nocturnal urban heat island: Comparison of scale model and field observations. *Journal of Climatology*, **1 (3)**, 237–254, doi:10.1002/joc.3370010304, URL http://dx.doi.org/10.1002/joc.3370010304.

Peter, H. and Schmid, 2002: Footprint modeling for vegetation atmosphere exchange studies: a review and perspective. *Agricultural and Forest Meteorology*, **113 (1-4)**, 159 – 183, doi:10.1016/S0168-1923(02)00107-7, URL http://www.sciencedirect.com/science/article/pii/S0168192302001077, ¡ce:title¿FLUXNET 2000 Synthesis¡/ce:title¿.

Schmid, H. P., 1994: Source areas for scalars and scalar fluxes. *Boundary-Layer Meteorology*, **67**, 293–318, URL http://dx.doi.org/10.1007/BF00713146, 10.1007/BF00713146.

Sundborg, A., 1950: Local climatological studies of the temperature conditions in an urban area. *Tellus*, **2 (3)**, 222–232, doi:10.1111/j.2153-3490.1950.tb00333.x, URL http://dx.doi.org/10.1111/j.2153-3490.1950.tb00333.x.

Unger, J., 2006: Modelling of the annual mean maximum urban heat island using 2d and 3d surface parameters. *Climate Research*, **30**, 215–226.

Van der Zon, N., 2011: Kwaliteitsdocument ahn-2, release 1.1. Release 1.1, Rijkswaterstaat Data-ICT-Dienst, Delft, the Netherlands.

WMO, 2008: Guide to meteorological instruments and methods of observation. WMO-No.8 8, WMO, Geneva, Switzerland.